eXPRESS Polymer Letters Vol.5, No.9 (2011) 825–837
Available online at www.expresspolymlett.com
DOI: 10.3144/expresspolymlett.2011.81

Sonochemical-assisted fabrication of biologically active chiral poly(ester-imide)/TiO_2 bionanocomposites derived from L-methionine and L-tyrosine amino acids

S. Mallakpour[1,2*], *F. Zeraatpisheh*[1], *M. R. Sabzalian*[3]

[1]Organic Polymer Chemistry Research Laboratory, Department of Chemistry, Isfahan University of Technology, Isfahan, 84156-83111, I. R. Iran
[2]Nanotechnology and Advanced Materials Institute, Isfahan University of Technology, Isfahan, 84156-83111, I. R. Iran
[3]College of Agriculture, Department of Agronomy and Plant Breeding, Isfahan University of Technology, Isfahan, 84156-83111, I. R. Iran

Received 30 December 2010; accepted in revised form 28 March 2011

Abstract. A new chiral poly(ester-imide) (PEI) was prepared via direct polyesterification of *N,N′*-(pyromellitoyl)-bis-(L-tyrosine dimethyl ester) and *N*-trimellitylimido-L-methionine using tosyl chloride/pyridine/*N,N′*-dimethylformamide system as a condensing agent. The resulting new chiral polymer was obtained in good yield and had good thermal stability as well as good solubility in common organic solvents. After that, PEI/titanium bionanocomposites (PEI/TiO_2 BNCs) were prepared using the modified nanosized TiO_2 via sonochemical reaction that can accelerate hydrolysis, increase collision chance for the reactive system and improve the dispersion of the nanoparticles in polymer matrix. The scanning electron microscopy (SEM), field emission scanning electron microscopy (FE-SEM) and transmission electron microscopy (TEM) results indicated that there is no aggregation of a large quantity of particles. Thermogravimetric analysis (TGA) confirmed that the heat stability of the BNC polymers in the temperature range of 400–800ºC was enhanced by addition of TiO_2 nanoparticles. Furthermore, in vitro toxicity test was employed for assessing the sensitivity of these compounds to microbial degradation. To this purpose, polymer and PEI/TiO_2 BNCs were investigated under soil burial conditions. The results of this study revealed that polymer and its BNCs are biologically active and non-toxic in the natural environment although some antimicrobial properties were found for BNCs.

Keywords: *biocomposites, non-toxic, TiO_2 nanoparticles, thermally stable poly(ester-imide), ultrasonic irradiation*

1. Introduction

The last decade has seen the improvement of an alternative chemistry, which intends to decrease the human impact on the environment. The biopolymers are noticeably involved in this tendency. However, even if much commercial merchandise is attainable, their current properties (mechanical properties and moisture sensitivity) have to be improved to be truly competitive with the petroleum-based products [1]. One of the most promising responses to conquer these weaknesses is designing bionanocomposites (BNC)s consisting of a biopolymer matrix reinforced with nanoparticles having at least one dimension in the nanometer range (1–100 nm) [2]. These hybrid materials combine the advantages of the organic biopolymers (light weight, flexibility, good impact resistance, good processability and biodegradability) and inorganic nanofiller materials (good chemical resistance, high thermal stability, and high brittleness). Thus they create several industrial applications [3–5]. For producing suitable BNCs, it is necessary to

*Corresponding author, e-mail: mallak@cc.iut.ac.ir

disperse the inorganic materials such as nanoparticles in organic matrices. A homogeneous dispersion of the nanoparticles is believed to contribute better to the property enhancement. However, nanoparticles aggregate easily and difficult to disperse them in a solvent or polymer matrix because of their high specific surface area and surface energy. Some technical routes, such as encapsulating polymerization [6], solution intercalation [7], latex precompounding [8], ultrasonic irradiation [9] and the use of different coupling agents [10] were developed for enhancing the dispersion state of nanoparticles in polymer matrix. However, the sonochemical method has been reported to be faster than aforementioned techniques. The main advantage in sonochemical experiments is that it is rather inexpensive. Sonochemistry, the chemical effects of high intensity ultrasound, is a topic of resurging interest for its biological, synthetic and catalytic relevance. Ultrasonic irradiation arisen from acoustic cavitation can produce hot spots with transient temperatures of about 5000 K, and local pressure as high as 500 atm in a very rigorous environment. Hence, the utilization of ultrasound to improve the rate of reaction has become a routine method in scattering, crushing, and activation of particles, as well as initiation of polymerization [9, 11–14].

Among many inorganic nanoparticles, nanosized titanium dioxide (TiO_2) is one of the most encouraging inert, nontoxic, and cheap materials in research because of its versatile functions such as antifouling, antimicrobial, deodorizing and photovoltaic effects [15]. Therefore, it has a widespread range of applications, e.g. in filters, lenses, reflectors, optical adhesives and antireflection films [16–18], optical waveguides [19], photochemical solar cells [20], and TiO_2-based photocatalytic detoxification of air and water for environmental remediation [21–24].

Owing to the escalating performance characteristics demanded on polymers in various fields, use of poly(ester-imide)s (PEI)s because of favorable properties, such as good heat resistance, mechanical strength, electrical insulation and other physical properties are growing steadily. As a matter of fact, PEI is the combination of polyimide and polyester which could have properties of both of them and provides good balance between thermal stability and processability [25–26]. Among the PEIs, chiral ones are important polymers in macromolecular science. In general, the synthesis of optically active synthetic polymers is a subject of special interest because of their applications to chromatographic supports, catalysts and materials with ferroelectric and nonlinear optical properties. The optical activity of the polymer can be tuned by choosing a suitable chiral initiator or by starting from a chiral monomer [27].

In this work, a novel PEI containing L-methionine and L-tyrosine amino acids in the main chain was prepared via direct polycondensation reaction. Then, optically active PEI/TiO_2 BNCs were synthesized through a simple and convenient ultrasonic wave dispersion process of modified nanoparticle with coupling agent. The resulting BNC polymers are characterized by several techniques including Fourier transform infrared spectroscopy (FT-IR), powder X-ray diffraction (XRD), thermogravimetric analysis (TGA) and their morphology were investigated by field emission scanning electron microscopy (FE-SEM), scanning electron microscopy (SEM) and transmission electron microscopy (TEM) analysis.

2. Experimental

2.1. Materials

All chemicals were purchase from Fluka Chemical Co. (Buchs, Switzerland), Aldrich Chemical Co. (Milwaukee, WI), Riedel-deHaen AG (Seelze, Germany) and Merck Chemical Co. *N,N*′-Dimethyformamide (DMF) and pyridine (Py) were dried over barium oxide (BaO) and then were distilled under reduced pressure. The coupling agent (3-aminopropyltriethoxysilane) (KH550), was obtained from Merck Chemical Co. Nanosized TiO_2 powder which contain mostly anatase form with small percentage of rutile form was purchased from Nanosabz Co. with average particle sizes of 30–50 nm. The amino acids were used as obtained without further purification.

2.2. Characterization

Infrared spectra of the samples were recorded at room temperature in the range of 4000–400 cm^{-1}, on (Jasco-680, Japan) spectrophotometer. The spectra of solids were obtained using KBr pellets. The vibrational transition frequencies are reported in wave numbers [cm^{-1}]. Band intensities are assigned as weak (w), medium (m), strong (s) and broad (br).

Proton nuclear magnetic resonance (^{1}H-NMR spectra, 500 MHz) were recorded in *N,N′*-dimethylsulfoxide (DMSO)-d_6 solution using a Bruker (Germany) Avance 500 instrument. Multiplicities of proton resonance were designated as singlet (s) and multiplet (m). Inherent viscosity was measured by a standard procedure with a Cannon-Fenske (Mainz, Germany) routine viscometer. Specific rotation was measured with a Jasco (Osaka, Japan) P-1030 polarimeter at the concentration of 0.5 g/dl at 25ºC. TGA data were taken on STA503 WinTA instrument in a nitrogen atmosphere at a heating rate of 10ºC/min. Elemental analyses were performed by Leco, CHNS-932. The XRD patterns of the polymer and BNC polymers were recorded by employing a Philips X'PERT MPD diffractometer with a copper target at 40 kV and 30 mA and Cu K_α radiation: $\lambda = 1.54$ Å in the range 10–80º at the speed of 0.05º/min. To clarify the nanoscale structure, TEM (CM 120, Philips) was also used, at an accelerating voltage of 100 kV. For TEM, BNCs were suspended in water and a small drop of suspension was deposited on the carbon coated copper grid. SEM measurements of polymer and BNC polymers were carried out on a Philips XLC with backscattered electron detector at voltage of 20 kV. Small pieces of samples were mounted onto stubs using adhesive tapes and sputtered with a gold layer. Surface morphology and sample homogeneity of BNC polymers were characterized using FE-SEM (JSM-6700F, Japan).

2.3. Apparatus

The reaction was occurred on a MISONIX ultrasonic liquid processor, XL-2000 SERIES. Ultrasonic irradiation was carried out with the probe of the ultrasonic horn immersed directly in the mixture solution system with frequency of $2.25 \cdot 10^4$ Hz and 100 W powers.

2.4. Monomer synthesis

N-Trimellitylimido-L-methionine 1 as a diacid and *N,N′*-(pyromellitoyl)-bis-L-tyrosine dimethyl ester 2 as a diphenolic monomer were prepared according to our previous works [28, 29].

2.5. Polymer synthesis

The PEI was prepared by the following procedure and is shown in Figure 1. A solution of Py (0.20 ml) with tosyl chloride (TsCl) (0.29 g; $1.55 \cdot 10^{-3}$ mol) after 30 min stirring at room temperature, was treated with DMF (0.09 ml; $1.22 \cdot 10^{-3}$ mol) for 30 min and the mixture was added dropwise to a solution of diacid (2) (0.10 g; $3.09 \cdot 10^{-4}$ mol) in Py (0.20 ml). The mixture was maintained at room temperature for 30 min and then diol (1) (0.18 g; $3.09 \cdot 10^{-4}$ mol) was added to this mixture and the whole solution was stirred at room temperature for

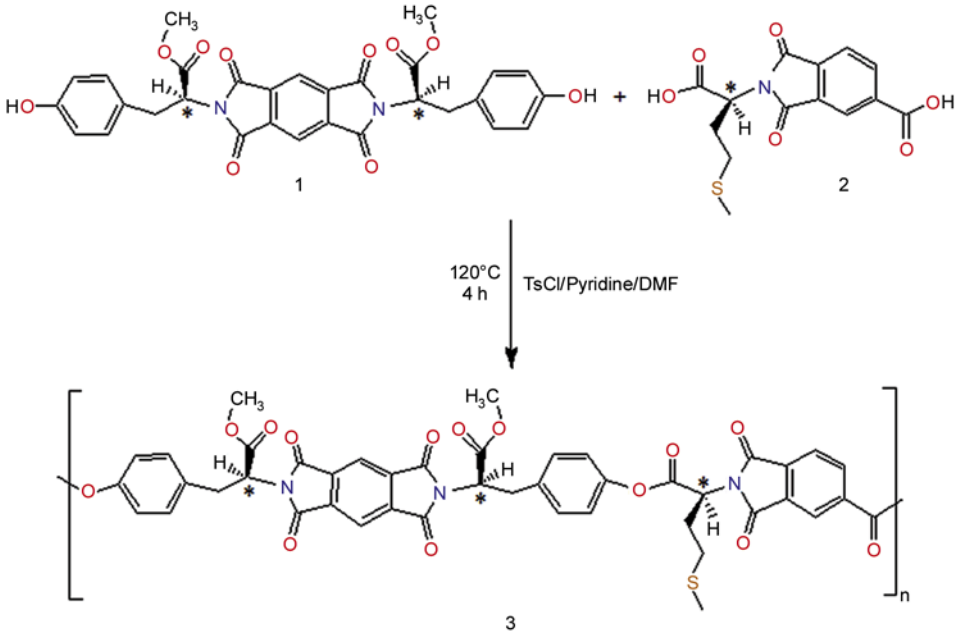

Figure 1. Synthesis of the PEI [3]

30 min and then at 120ºC for 4 h. As the reaction proceeded, the solution became viscous and then the viscous liquid was precipitated in 30 ml of methanol to give 0.24 g pale brown powder PEI (93% yield) and the specific rotation was measured ($[\alpha]_D^{25} = +18$).

FT-IR Peaks (KBr, cm^{-1}): 3433 (w, br), 3035 (w), 3070 (w), 2921 (m), 2852 (w), 1777 (s), 1722 (s), 1508 (m), 1382 (s), 1279 (w), 1245 (m), 1196 (m), 1169 (m), 1112 (w), 1099 (w), 727 (m).

^{1}H-NMR (500 MHz, DMSO-d_6, δ, ppm): 1.96 (s, 3H), 2.28–2.36 (m, 2H), 2.58–2.63 (m, 2H), 3.00–3.54 (m, 4H), 3.67 (s, 6H), 5.31 (m, 4H), 6.85 (s, 2H, Ar–H), 7.09-7.17 (m, 4H, Ar–H), 7.26 (s, 2H, Ar–H), 8.02 (s, 1H, Ar–H) 8.13–8.23 (m, 2H, Ar–H), 8.33(s, 1H, Ar–H), 8.42 (s, 1H, Ar–H).

Elemental analysis: calcd. for ($C_{44}H_{33}N_3O_{14}S$): C, 61.32%; H, 4.09%; N, 4.88%; S, 3.72%. Found: C, 60.20%; H, 4.27%; N, 5.11%; S, 3.96%.

2.6. Preparation of PEI/TiO_2 BNCs through ultrasonic irradiation

TiO_2 nanoparticles were chemically modified using ultrasonic reaction to obtain the KH550-capping TiO_2 particles. Typically, TiO_2 nanoparticles (0.30 g) were added into acetone (10 ml), and 10% weight percentage of KH550 was dissolved in H_2O (10 ml). The mixture was then exposed to high-intensity ultrasound irradiation for 30 min. After that it was centrifuged and dried. PEI was dispersed in 20 ml of absolute ethanol. A uniform colloidal dispersion was obtained after ultrasonication for 15 min at room temperature. The suspension was mixed with the appropriate amount of TiO_2-KH550 powder to produce 5, 10, 15, 20 and 25% W/W based on the PEI content followed by irradiation with high-intensity ultrasonic wave for 4 h at room temperature [30, 31]. After irradiation, the resulting suspension was centrifuged, and the precipitate was washed twice

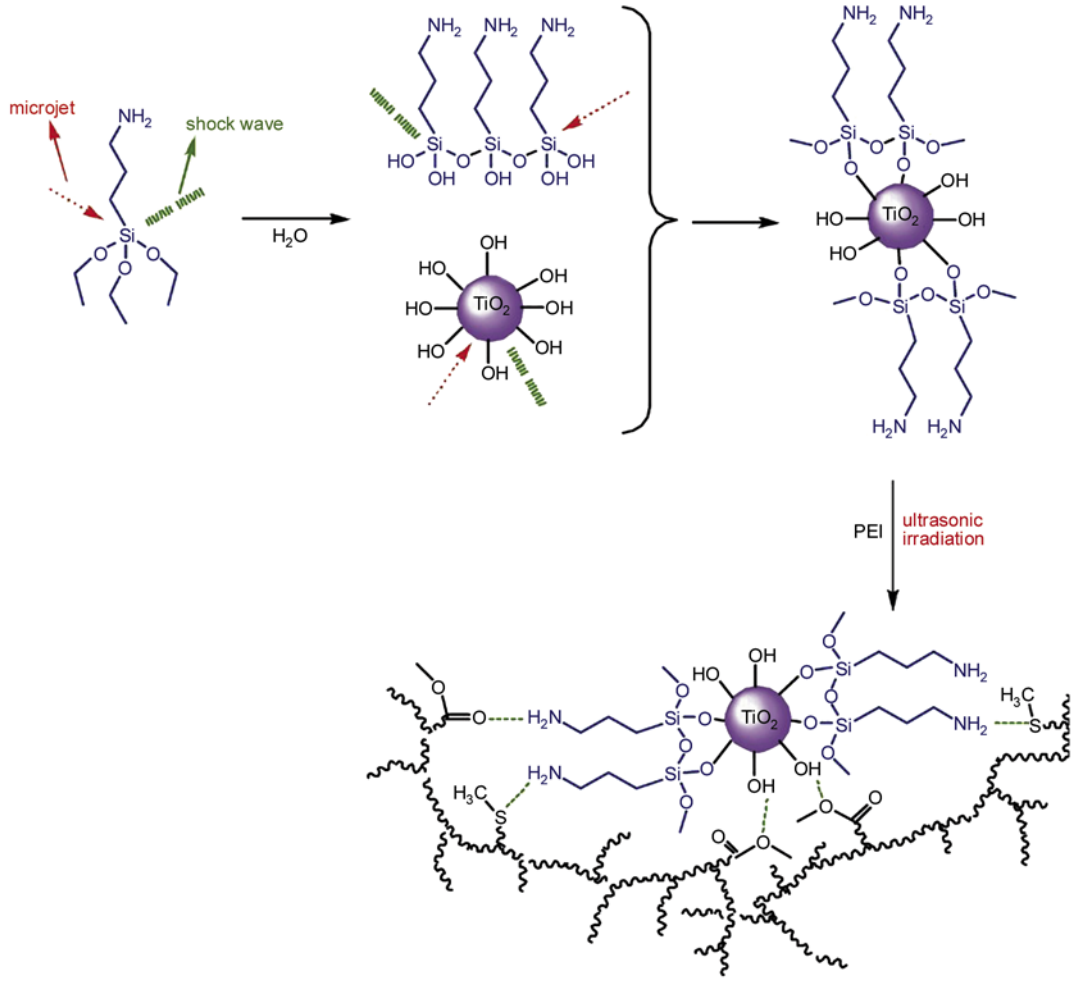

Figure 2. Preparation of PEI/TiO_2 BNCs

with absolute ethanol. The solid was dried in vacuum at room temperature for 8 h and the obtained product was kept for further characterization. The process is described in Figure 2.

2.7. Soil burial test of PEI/TiO_2 BNCs

The bioactivity of the PEI/TiO_2 BNCs was checked during natural soil burial for 3 months. Thirty-mg specimens of diacid, and obtained polymers of PEI and PEI/TiO_2 BNC (10 wt%) were buried in the soil by mixing with 1.5 g clay-loam soil in 1.5 ml plastic vials. Samples were incubated at almost constant temperature of 28°C for three months. The moisture content was maintained at 60–70% of the soil maximum water holding capacity. Also, the vials were capped to avoid water evaporation from the soil surface. After 90 days, the buried specimens were dug out, immersed in distilled water and water extracts of samples were inoculated on Potato Dextrose Agar (PDA) medium by streak culture and soil microbial population as the number of bacterial and fungal colony forming units (CFUs) per 100 µl of water extract was counted. Soil free of any compound and BPA-containing soil were used as negative and positive control, respectively, for comparison.

2.8. Effect of PEI/TiO_2 BNCs on growth of wheat seedlings

Plastic vials with capacity of 1.5 ml were used, each receiving 30 mg of each compound including diacid, obtained polymer and PEI/TiO_2 BNC (10 wt%) in three replications. Vials were incubated at 23–25°C, with a saturated humidity at dark for 3 months. After this period, wheat seeds were pre-germinated on distilled water humidified germination paper, during a period of five days in a germination chamber under controlled conditions (temperature of 25ºC and photoperiod light and dark of 14/10 h). Then, an individual germinated wheat seed was put on the soil in the center of each vial so that rootlet was in contact with soil. Seedlings were grown in a glass box with 80% humidity and observations were made on seedling growth. Plants were harvested 20 days after transplanting. Shoot length was measured using a ruler, and then seedlings were dried at 65ºC for 48 h for total dry matter measurement.

3. Results and discussion

3.1. Polymer synthesis

PEI was synthesized by the direct polycondensation reaction of an equimolar mixture of diol 1 with diacid 2 in a system of TsCl/Py/DMF as condensing agent (Figure 1). For the polycondensation of aromatic diacid and aromatic diol, a vilsmeier adduct was prepared by dissolving TsCl in a mixed solvent of Py and DMF. Polyesterifacation of diacid with aromatic diol was carried by varying the aging time of the initial reaction of TsCl and Py. TsCl was dissolved in Py at room temperature and kept at this temperature for 30 min according to previously reported procedures that the suitable aging time is 30 min [32]. It was determined that a molar ratio of diacid over TsCl equal to 5 and the reaction time of 4 h are required to produce a polymer with better yield and inherent viscosity. Further addition of TsCl did not improve the inherent viscosity of polymer and also caused the diminution of yield. The reaction was also run at 120°C as proposed by Higashi *et al.* [33]. The inherent viscosity of the resulting polymer under optimized condition was 0.41 dl/g and the yield was 93%. The incorporation of chiral units into the polymer backbone was obtained by measuring the specific rotation of polymer which show optical rotation and therefore is optically active ($[\alpha]_D^{25} = +18$). For that reason, this polymer has potential to be used as chiral stationary phase in HPLC for the separation of racemic mixtures. The resulting polymer is readily soluble in many organic solvents such as *N,N*′-dimethylacetamide (DMAc), *N*-methyl-2-pyrrolidone (NMP), DMSO and DMF. This optically active polymer is expected to be used as a biomaterial because of the presence of ester linkages and amino acids in its architecture.

3.2. Polymer characterization

The resulting polymer was characterized by FT-IR, ^{1}H-NMR spectroscopy techniques and elemental analyses. The FT-IR spectrum of PEI (Figure 3, curve c) exhibited characteristic absorptions of imide and ester groups around 1777 and 1722 cm^{-1}, which are related to carbonyls stretching of imide and ester groups, respectively. The peaks at 1382 and 727 cm^{-1} show the presence of the imide heterocy-

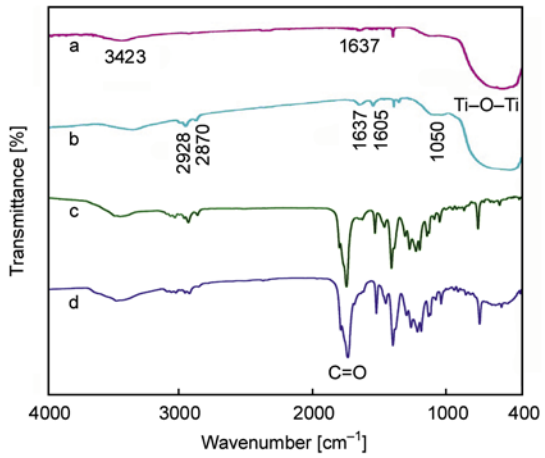

Figure 3. FT-IR spectra of (a) pure TiO_2 nanoparticles, (b) TiO_2 nanoparticles modified by KH550 (c) pure PEI (d) PEI/TiO_2 BNC (10 wt%)

cle in this polymer. The ^{1}H-NMR spectrum (500 MHz) of PEI is shown in Figure 4. In the ^{1}H-NMR spectrum of this polymer, the appearance of the methoxy protons (OCH_3) at 3.67 ppm as single peak indicates the presence of ester groups in the polymers side chain. The protons of the three chiral centers appeared at 5.31 ppm. The resonance of the diastereotopic hydrogens bonded to neighbor carbon of chiral centers appeared in the 2.58–2.63 and 3.00–3.54 ppm. The resonance of aromatic protons appeared in the range of 6.85–8.42 ppm. Elemental analysis values of the resulting polymer are also in good agreement with calculated values of carbon, hydrogen, nitrogen and sulfur in the polymer.

3.2.1. Preparation of PEI/TiO_2 BNCs

Nanoparticles have a strong tendency to agglomerate because of their high surface energy. To break down the nanoparticles agglomerates and improving the dispersivity of nanosized TiO_2 in polymer matrix, in this study, ultrasonic irradiation was employed to synthesize the BNC polymers. However, this approach will be restricted due to the limited interaction between the inorganic materials and the polymeric matrix, compared with the very strong interaction between individual nanoparticles. To attain proper dispersion of nanoparticles within polymer matrix and to yield a better compatibility between the nanoparticles and host polymeric materials, surface-modification is used for producing nanostructural composites.

The sonochemical reaction supplies appropriate reaction temperature to accelerate the hydrolysis of KH550. Furthermore, the microjets and shock waves created by intense ultrasonic waves in solution play a significant role in the combination of hydrolyzed KH550 and TiO_2 sol. In this condition, the collision chance of KH550 anchored onto the

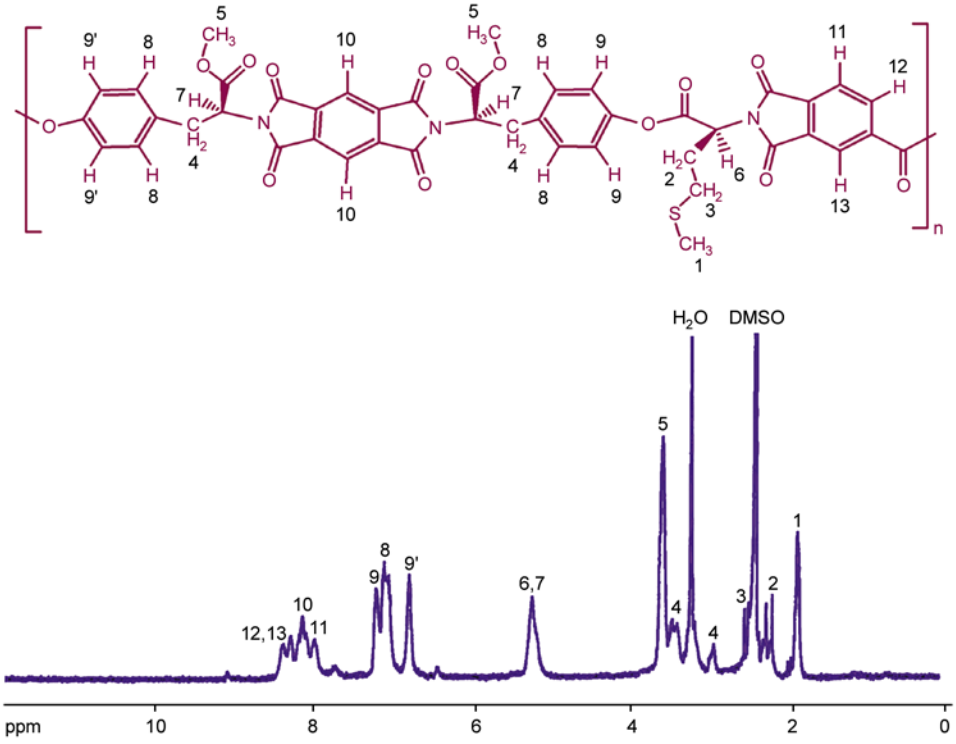

Figure 4. ^{1}H-NMR (500 MHz) spectrum of PEI in DMSO-d_6

surface of TiO_2 sol particles is greatly increased [34]. Silanol groups of KH550 generated by hydrolysis can interact with hydroxyl groups on the TiO_2 surface and form the modification layer with $–NH_2$ groups. Inasmuch the resulting PEI has lots of polar groups such as carbonyl, nitrogen and sulfur; the modified nanoparticles might be dispersed absolutely and will combine with PEI by different connections such as hydrogen bond, and also short-ranged steric and electrical interactions [35]. The details of the fabrication mechanism are displayed in Figure 2. Dispersion of nanoparticles in the polymer matrix can be observed from the photographs of TEM, FE-SEM and SEM.

3.2.2. Infrared study

FT-IR spectroscopy studies yielded useful qualitative information on the PEI/TiO_2 BNCs. Figure 3 shows the infrared spectra of pure TiO_2 nanoparticles (a), KH550-modified-TiO_2 (b), pure PEI (c) and PEI/TiO_2 BNC (10 wt%) (d). In the spectrum of pristine TiO_2, OH stretching band and bending band are observed at 3423 and 1637 cm^{-1}, respectively. The observed broader bands at 3500 and 3422 cm^{-1} were attributed to hydroxyl groups on different sites and some varying interactions between hydroxyl groups on TiO_2, respectively [31]. A broad absorption peak at 500–800 cm^{-1} is assigned to the Ti–O–Ti stretching band. As a result, the presence of KH550 on the surface of TiO_2 was confirmed by the characteristic peaks of CH stretching band at 2870–2928 cm^{-1} in the infrared data of KH550-modified-TiO_2 nanoparticles compared to the infrared data of pure TiO_2. The N–H bending vibration of primary amine is observed around 1605 cm^{-1}. In addition, the broad band around 1050 cm^{-1} corresponded to Si–O–Si bond is observed which indicates the condensation reaction between silanol groups. It is assumed that KH550 is adhering to the nano-TiO_2 particles possibly by coating. FT-IR spectrum of PEI/TiO_2 BNC (10 wt%) is shown in Figure 3d, where the characteristic peaks of pure PEI and TiO_2 are still maintained, it may be proved that the structure of PEI was affected by the presence of TiO_2.

FT-IR spectra of BNC polymers with different amounts of TiO_2 (5, 10, 15, 20, 25 wt%) nanoparticles (Figure 5) shows the intensity of Ti–O–Ti stretching band raise with an increase of TiO_2 nanoparticles content in PEI.

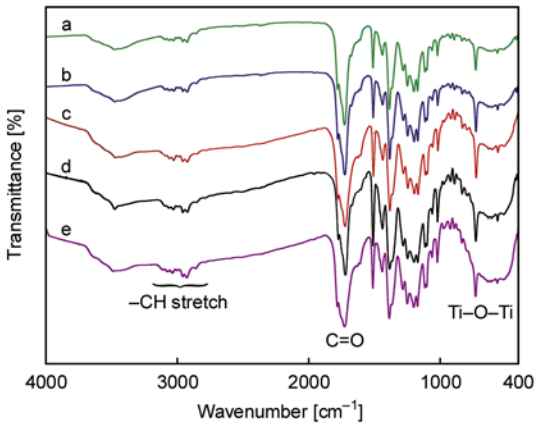

Figure 5. FT-IR spectra of (a) PEI/TiO_2 BNC (5 wt%), (b) PEI/TiO_2 BNC (10 wt%), (c) PEI/TiO_2 BNC (15 wt%), (d) PEI/TiO_2 BNC (20 wt%), (e) PEI/TiO_2 BNC (25 wt%)

3.2.3. X-ray diffraction data

XRD curves of PEI (a), pure TiO_2 (b), PEI/TiO_2 BNC (5 wt%) (c) and PEI/TiO_2 BNC (10 wt%) (d) are shown in Figure 6. The broad peak in the region of $2\theta = 10–30°$ in XRD curve of PEI shows that PEI prepared in the absence of TiO_2 nanoparticles is amorphous. Figure 6 (b) shows anatase and rutile phase for pure TiO_2 nano particles. The XRD patterns of PEI/TiO_2 BNC (c) and (d) show characteristic peaks of anatase and rutile of TiO_2 indicating that the crystallinity form of TiO_2 nanoparticles has

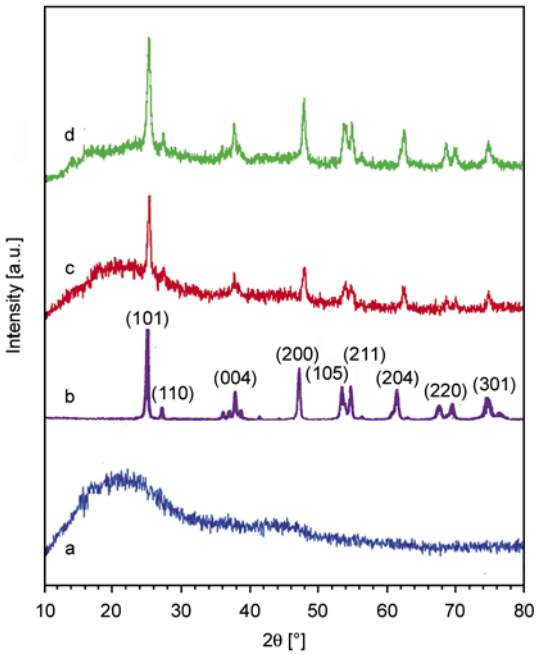

Figure 6. XRD curves of (a) PEI (b) pure TiO_2 nanoparticles (c) PEI/TiO_2 BNC (5 wt%), (d) PEI/TiO_2 BNC (10 wt%)

not been disturbed during the process. Also, the broad weak diffraction peak of PEI still exists, but its intensity decreases. It implies that the composite sample has a more ordered arrangement than the bare polymer owing to the TiO_2.

The average crystalline size of nano-TiO_2, which is determined from the half-width of the diffraction using the Debye–Scherrer equation, is approximately 20 nm for PEI/TiO_2 BNC (10 wt%) and 16 nm for PEI/TiO_2 BNC (5 wt%). Sherrer's Equation (1) is as follows:

$$D = \frac{0.9\lambda}{\beta\cos\theta} \quad (1)$$

where D is the crystallite size, λ is wavelength of the radiation, θ is the Bragg's angle and β is the full width at half maximum [36].

3.2.4. Morphology observation

SEM micrograph (Figure 7) of the PEI containing no TiO_2 nanoparticles is shown in Figure 7a. It has a surface with no evidence of surface topography observed at the magnification used during SEM observations. Representative SEM images of PEI/TiO_2 BNC (5 wt%) (b, c) and PEI/TiO_2 BNC (10 wt%) (d) as well as FE-SEM pictures of PEI/TiO_2 BNC (10 wt%) are exhibited in Figure 8 and presented a homogeneous microstructure and con-

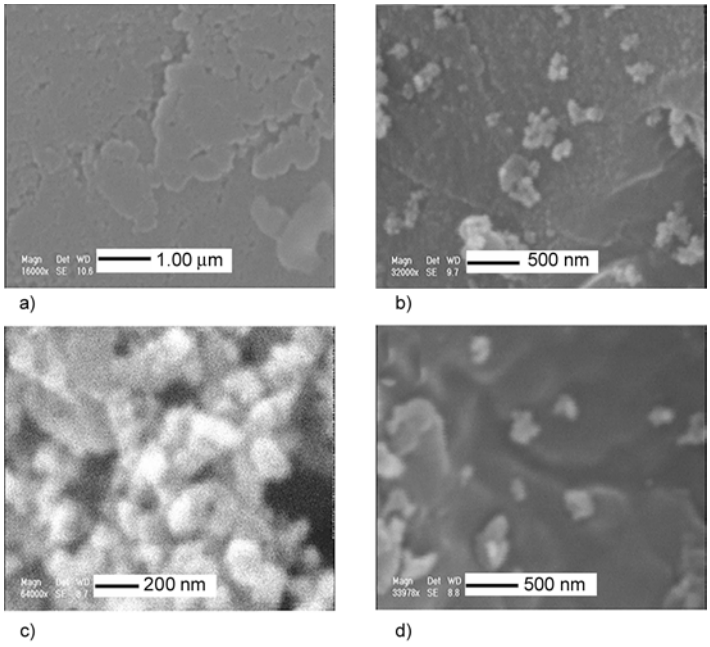

Figure 7. SEM micrographs of pure PEI (a), PEI/TiO_2 BNC (5 wt%) (b, c), PEI/TiO_2 BNC (10 wt%) (d)

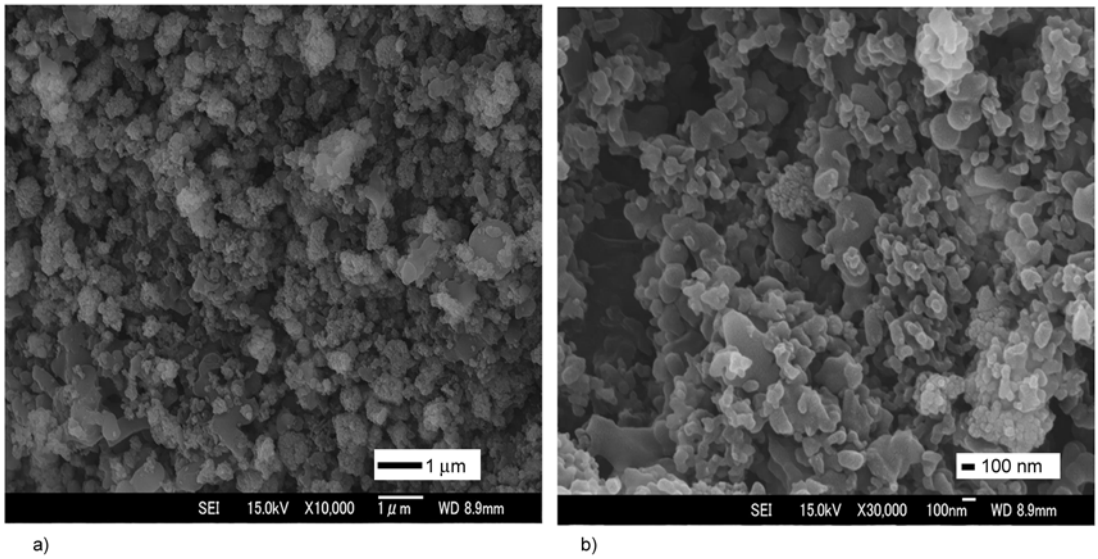

Figure 8. FE-SEM micrographs of PEI/TiO_2 BNC (10 wt%)

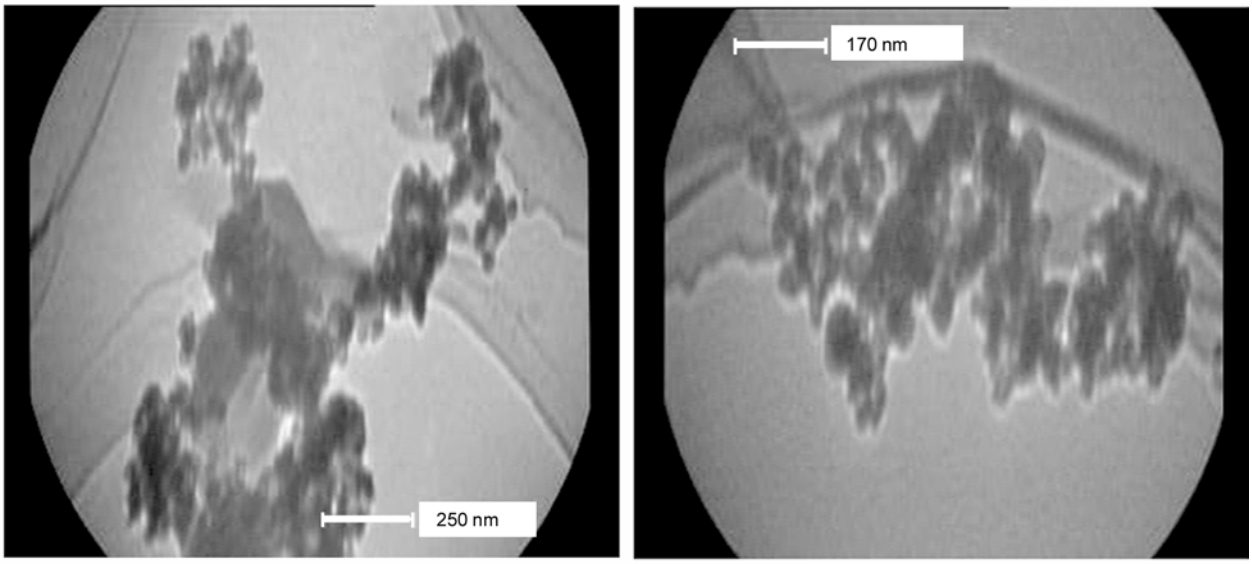

Figure 9. TEM micrographs of PEI/TiO_2 BNC (5 wt%)

firmed that the TiO_2 nanoparticles appear on the PEI surface in nanoscale comparing with surface of pure PEI.

Figure 9 shows the morphology of PEI/TiO_2 BNC (5 wt%) as obtained by TEM micrographs which demonstrated some distinctive domains and dispersion of TiO_2 nanoparticles (about 50 nm) in the PEI matrix.

3.3. Thermal properties

Thermogravimetric analysis was applied to evaluate the thermal properties of the PEI and PEI/TiO_2 BNCs at a heating rate of 10ºC/min, under a nitrogen atmosphere. Figure 10 demonstrates the respective TGA profiles and the corresponding thermoanalysis data, including the temperatures at which 5% (T_5) and 10% (T_{10}) degradation occur. Char yield at 800ºC and also limiting oxygen index (LOI) based on Van Krevelen and Hoftyzer equation (Equation (2)) are summarized in Table 1 [37]:

$$LOI = 17.5 + 0.4\ CR \quad (2)$$

where CR = char yield.

From these data it is clear that the PEI is stable to 300ºC and introduction of inorganic nanoparticles in polymer matrix induced the thermal properties to rise. However, the initial temperature of the bionanocomposites weight loss was not increased considerably with increasing TiO_2 content until at a weight loss of 40%. Increasing in the thermal stabil-

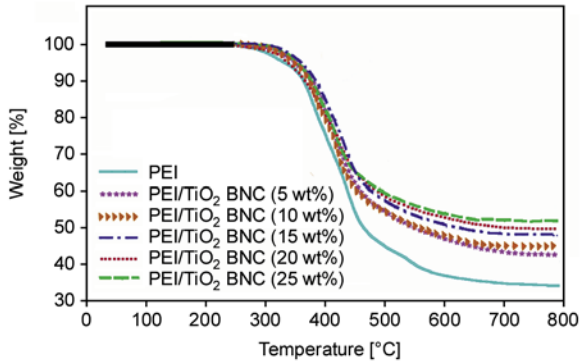

Figure 10. TGA thermograms of PEI and PEI/TiO_2 BNCs under a nitrogen atmosphere at heating rate of 10°C/min

Table 1. Thermal properties of the PEI and PEI/TiO_2 BNCs

Samples	T_5 [°C][a]	T_{10} [°C][b]	Char Yield [%][c]	LOI[d]
PEI	328	360	34	31.1
PEI/TiO_2 BNC (5 wt%)	346	370	43	34.7
PEI/TiO_2 BNC (10 wt%)	347	368	45	35.5
PEI/TiO_2 BNC (15 wt%)	355	378	48	36.7
PEI/TiO_2 BNC (20 wt%)	337	363	49	37.1

[a]Temperature at which 5% weight loss was recorded by TGA at heating rate of 10°C/min under a nitrogen atmosphere.
[b]Temperature at which 10% weight loss was recorded by TGA at heating rate of 10°C/min under a nitrogen atmosphere.
[c]weight percentage of material left undecomposed after TGA analysis at a temperature of 800°C under a nitrogen atmosphere.
[d]Limiting oxygen index (LOI) evaluating char yield at 800°C.

ity may happen as an effect of the high thermal stability of TiO_2 network and the physical crosslink points of the TiO_2 particles, which may restrict the movement of the molecular chain of PEI. Subsequent to addition of TiO_2 nanoparticles with high melting point to the polymer matrix, the TiO_2 particles can serve as a good thermal cover layer, avoiding the direct thermal decomposition of polymer matrix by heat. Also, TiO_2 nanoparticles offer a larger surface area and enhance the effect of thermal cover [38, 30]. The char yield of pure PEI at 800ºC is 34%, whilst those of the bionanocomposites (PEI/TiO_2 BNC 5, 10, 15, 20, 25 wt%) at 800ºC are in the range of 43–52%, and this increases with an increase of TiO_2 nanoparticles content in the PEI. On the basis of LOI values (34–38), all macromolecules can be classified as self-extinguishing BNC polymers.

3.4. Soil burial study

The enzymatic biodegradation of a polymer depends on the microbial populations, the pH-value, temperature, moisture, low glass temperature (high mobility), and low crystallinity. Therefore higher microbial population could be correlated to higher biodegradation. A lower colonial growth of bacteria and fungi was observed from water extract of soil containing PEI/TiO_2 BNC (10 wt%) compared with PEI (Figures 11 and 12). This result may indicate that degradation of PEI should be faster than PEI/TiO_2 BNC (10 wt%) because the former is more attacked by microorganisms. This was confirmed by higher colony count of bacteria and fungi on the media of PEI water extract compared with control soil and soil containing toxic BPA (Table 2). Evidently, this may suggest slight antimicrobial activity of PEI/TiO_2 BNC buried in the soil. Some other experiments also showed that the antimicrobial activity of the nano-TiO_2 composites increases with increasing concentration [39] and higher antimicrobial behavior will reduce biodegradation of the polymer in the soil. It may be recommended that for synthesis of biocompatible polymers, low concentration of TiO_2 must be used.

3.5. Wheat growth bioassay

The total dry matter provides the best indication of an adverse plant response to toxic substances and it

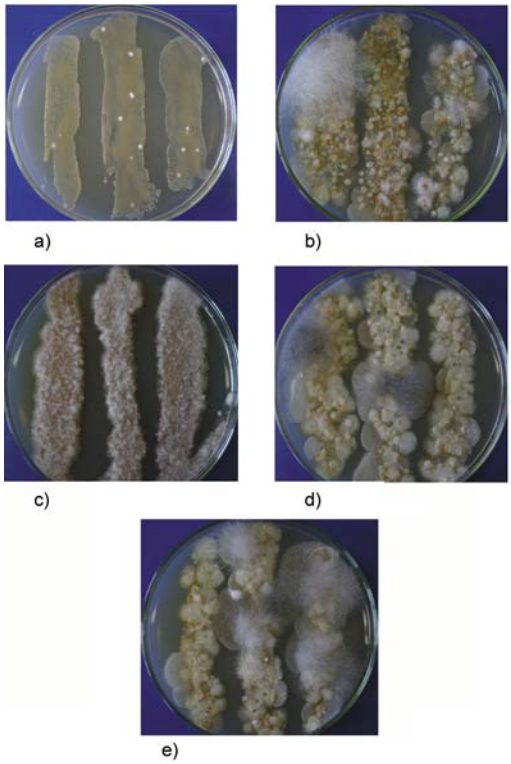

Figure 11. Fungal colonies grown from water extract of the soil containing diacid (c), PEI (d) and PEI/TiO_2 BNC (10 wt%) (e) compared with BPA (a) and control soil (b) on PDA Petri plates

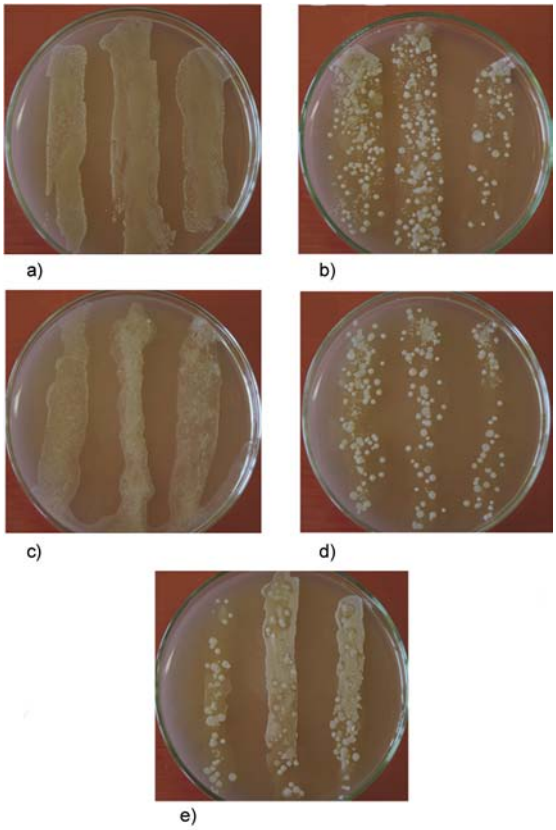

Figure 12. Bacterial colonies grown from water extract of the soil containing diacid (c), PEI (d) and PEI/TiO_2 BNC (10 wt%) (e) compared with BPA (a) and control soil (b) on PDA Petri

Table 2. The number of bacterial and fungal colonies (CFUs) from water extract of soil containing diacid, PEI and PEI/TiO_2 BNC grown on PDA Petri plates compared with control treatments

Compound	Fungal colony forming units (CFUs) [n/100 µl]	Bacterial colony forming units (CFUs) [n/100 µl]
Diacid	193±14.0	0±0
PEI	49±2.5	102±6.6
PEI/TiO_2 BNC (10 wt%)	30±2.5	54±12.5
BPA	2±1.5	0±0
Negative control (soil)	30±2.5	88±28.5

Table 3. Effect of diacid (b), PEI (c) and PEI/TiO_2 BNC (10 wt%) (d) compared with control soil (a) on wheat seedlings height [mm] and seedling dry weight [mg]

Material	Control soil (a)	Diacid (b)	PEI (c)	PEI/TiO_2 BNC (10 %wt) (d)
Seedling height [mm]	188.0	176.0	192.0	162.0
Seedling weight [mg]	23.5	13.5	16.2	14.2

Figure 13. Effect of diacid (b), PEI (c) and PEI/TiO_2 BNC (10 wt%) (d) compared with control soil (a) on survival and growth of wheat seedlings

has been found that wheat is sensitive plant to toxicity of organic wastes in plant growth bioassays. The application of PEI/TiO_2 BNC (10 wt%) in the soil did not present significant negative effects on total dry matter production compared with PEI (Figure 13). However, compared to the control (Table 3), both compounds reduced total dry matter, and shoot length probably due to lower availability of nutritional elements. These results show that both PEI and PEI/TiO_2 BNC (10 wt%) probably have no toxicity for plant growth and are highly compatible with natural ecosystems providing low concentration of TiO_2 in polymer structure.

4. Conclusions

In summary, a new thermally stable and optically active PEI was synthesized by direct step-growth polycondensation of *N,N′*-(pyromellitoyl)-bis-(L-tyrosine dimethyl ester) as an optically active aromatic diol with *N*-trimellitylimido-L-methionine using TsCl/DMF/Py as a condensing agent. Ultrasonic process was applied as a profitable route for the modification of TiO_2 nanoparticles with KH550 followed by synthesis of the PEI/TiO_2 BNCs. TEM analysis showed dispersion of TiO_2 with average particle sizes about 50 nm in the polymer matrix. Also, morphological study of synthesized BNCs exhibited the TiO_2 nanoparticles mostly dispersed homogeneously on the polymer matrix by FE-SEM analysis. According to the LOI values, obtained BNC polymers can be categorized as self-extinguishing materials. FT-IR and XRD data also established that TiO_2 nanoparticles exist in the PEI matrix. The presence of natural amino acids in the PEI combined with bioactive TiO_2 nanoparticles made these BNC polymers capable to be potentially bioactive. To ensure real bioactivity and safe incorporation of these materials in the geochemical life cycle, in vitro soil burial and plant bioassay tests were performed. The results illustrated that synthesized polymers could be probably decomposed by soil microorganisms; however, the addition of TiO_2 resulted in a decrease in the microbial population due to its antimicrobial activity, and high biodegradability of PEI/TiO_2 BNC depends on low concentration of incorporated titanium dioxide.

Acknowledgements

We wish to express our gratitude to the Research Affairs Division Isfahan University of Technology (IUT), Isfahan, for partial financial support. Further financial support from Iran nanotechnology Initiative Council (INIC), National Elite Foundation (NEF) and Center of Excellency in Sensors and Green Chemistry Research (IUT) are gratefully acknowledged. We also extend our thanks to Dr. A. Ashrafi for his valuable discussion.

References

[1] Chivrac F., Pollet E., Avérous L.: Progress in nano-biocomposites based on polysaccharides and nano-oclays. Materials Science and Engineering R: Reports, **67**, 1–17 (2009).
DOI: 10.1016/j.mser.2009.09.002

[2] Kumar P., Sandeep K. P., Alavi S., Truong V. D., Gorga R. E.: Preparation and characterization of bio-nanocomposite films based on soy protein isolate and montmorillonite using melt extrusion. Journal of Food Engineering, **100**, 480–489 (2010).
DOI: 10.1016/j.jfoodeng.2010.04.035

[3] Guan C., Lü C-L., Liu Y-F., Yang B.: Preparation and characterization of high refractive index thin films of TiO_2/epoxy resin nanocomposites. Journal of Applied Polymer Science, **102**, 1631–1636 (2006).
DOI: 10.1002/app.23947

[4] Mallakpour S., Tirgir F., Sabzalian M. R.: Synthesis, characterization and in vitro antimicrobial and biodegradability study of pseudo-poly(amino acid)s derived from *N*,*N*′-(pyromellitoyl)-*bis*-l-tyrosine dimethyl ester as a chiral bioactive diphenolic monomer. Amino Acids, **40**, 611–621 (2011).
DOI: 10.1007/s00726-010-0686-0

[5] Tingaut P., Zimmermann T., Lopez-Suevos F.: Synthesis and characterization of bionanocomposites with tunable properties from poly(lactic acid) and acetylated microfibrillated cellulose. Biomacromolecules, **11**, 455–464 (2010).
DOI: 10.1021/bm901186u

[6] Bourgeat-Lami E., Espiard Ph., Guyot A.: Poly(ethyl acrylate) latexes encapsulating nanoparticles of silica: 1. Functionalization and dispersion of silica. Polymer, **36**, 4385–4389 (1995).
DOI: 10.1016/0032-3861(95)96843-W

[7] Ratna D., Divekar S., Samui A. B., Chakraborty B. C., Banthia A. K.: Poly(ethylene oxide)/clay nanocomposite: Thermomechanical properties and morphology. Polymer, **47**, 4068–4074 (2006).
DOI: 10.1016/j.polymer.2006.02.040

[8] Siengchin S., Karger-Kocsis J., Apostolov A. A., Thomann R.: Polystyrene–fluorohectorite nanocomposites prepared by melt mixing with and without latex precompounding: Structure and mechanical properties. Journal of Applied Polymer Science, **106**, 248–254 (2007).
DOI: 10.1002/app.26474

[9] Wang Q., Xia H., Zhang C.: Preparation of polymer/inorganic nanoparticles composites through ultrasonic irradiation. Journal of Applied Polymer Science, **80**, 1478–1488 (2001).
DOI: 10.1002/app.1239

[10] Xu X., Li B., Lu H., Zhang Z., Wang H.: The interface structure of nano-SiO_2/PA66 composites and its influence on material's mechanical and thermal properties. Applied Surface Science, **254**, 1456–1462 (2007).
DOI: 10.1016/j.apsusc.2007.07.014

[11] Suslick K. S., Hammerton D. A., Cline R. E.: Sonochemical hot spot. Journal of the American Chemical Society, **108**, 5641–5642 (1986).
DOI: 10.1021/ja00278a055

[12] Yu J., Zhou M., Cheng B., Yu H., Zhao X.: Ultrasonic preparation of mesoporous titanium dioxide nanocrystalline photocatalysts and evaluation of photocatalytic activity. Journal of Molecular Catalysis A: Chemical, **227**, 75–80 (2005).
DOI: 10.1016/j.molcata.2004.10.012

[13] Yu J. C., Yu J., Zhang L., Ho W.: Enhancing effects of water content and ultrasonic irradiation on the photocatalytic activity of nano-sized TiO_2 powders. Journal of Photochemistry and Photobiology A: Chemistry, **148**, 263–271 (2002).
DOI: 10.1016/S1010-6030(02)00052-7

[14] Samal S. S., Jeyaraman P., Vishwakarma V.: Sonochemical coating of Ag-TiO_2 nanoparticles on textile fabrics for stain repellency and self-cleaning- The Indian scenario: A review. Journal of Minerals and Materials Characterization and Engineering, **9**, 519–525 (2010).

[15] Chen J-H., Dai C-A., Chen H-J., Chien P-C., Chiu W-Y.: Synthesis of nano-sized TiO_2/poly(AA-*co*-MMA) composites by heterocoagulation and blending with PET. Journal of Colloid and Interface Science, **308**, 81–92 (2007).
DOI: 10.1016/j.jcis.2006.12.066

[16] Olshavsky M. A., Allcock H. R.: Polyphosphazenes with high refractive indices: Synthesis, characterization, and optical properties. Macromolecules, **28**, 6188–6197 (1995).
DOI: 10.1021/ma00122a028

[17] Beecroft L. L., Ober C. K.: Nanocomposite materials for optical applications. Chemistry of Materials, **9**, 1302–1317 (1997).
DOI: 10.1021/cm960441a

[18] Papadimitrakopoulos F., Wisniecki P., Bhagwagar D. E.: Mechanically attrited silicon for high refractive index nanocomposites. Chemistry of Materials, **9**, 2928–2933 (1997).
DOI: 10.1021/cm970278z

[19] Yoshida M., Prasad P. N.: Sol−gel-processed SiO_2/TiO_2/poly(vinylpyrrolidone) composite materials for optical waveguides. Chemistry of Materials, **8**, 235–241 (1996).
DOI: 10.1021/cm950331o

[20] Kran R. K., Srivasatava O. N.: On the synthesis of nanostructured TiO_2 anatase phase and the development of the photoelectrochemical solar cell. International Journal of Hydrogen Energy, **24**, 27–35 (1999). DOI: 10.1016/S0360-3199(98)00009-3

[21] Park H., Choi W.: Effects of TiO_2 surface fluorination on photocatalytic reactions and photoelectrochemical behaviors. Journal of Physical Chemistry B, **108**, 4086–4093 (2004). DOI: 10.1021/jp036735i

[22] Yu J., Xiang Q., Zhou M.: Preparation, characterization and visible-light-driven photocatalytic activity of Fe-doped titania nanorods and first-principles study for electronic structures. Applied Catalysis B: Environmental, **90**, 595–602 (2009). DOI: 10.1016/j.apcatb.2009.04.021

[23] Liu S., Yu J., Jaroniec M.: Tunable photocatalytic selectivity of hollow TiO_2 microspheres composed of anatase polyhedra with exposed {001} facets. Journal of the American Chemical Society, **132**, 11914–11916 (2010). DOI: 10.1021/ja105283s

[24] Minero C., Mariella G., Maurino V., Pelizzetti E.: Photocatalytic transformation of organic compounds in the presence of inorganic anions. 1. Hydroxyl-mediated and direct electron-transfer reactions of phenol on a titanium dioxide−fluoride system. Langmuir, **16**, 2632–2641 (2000). DOI: 10.1021/la9903301

[25] Li C-H., Chen C-C., Chen K-M.: Studies on the synthesis and properties of copolyesterimide. Journal of Applied Polymer Science, **52**, 1751–1757 (1994). DOI: 10.1002/app.1994.070521209

[26] Hsu T-F., Lin Y-C., Lee Y-D.: Synthesis and characterization of novel thermotropic liquid crystalline copoly (ester imide)s. Journal of Polymer Science Part A: Polymer Chemistry, **36**, 1791–1803 (1998). DOI: 10.1002/(SICI)1099-0518(199808)36:11<1791::AID-POLA13>3.0.CO;2-9

[27] Iannelli M., Alupei V., Ritter H.: Selective microwave-accelerated synthesis and polymerization of chiral methacrylamide directly from methacrylic acid and (*R*)-1-phenyl-ethylamine. Tetrahedron, **61**, 1509–1515 (2005). DOI: 10.1016/j.tet.2004.11.068

[28] Mallakpour S., Kolahdoozan M.: Preparation of new poly(amide–imide)s with chiral architectures via direct polyamidation reaction. Journal of Applied Polymer Science, **104**, 1248–1254 (2007). DOI: 10.1002/app.25747

[29] Mallakpour S., Tirgir F., Sabzalian M. R.: Synthesis and structural characterization of novel biologically active and thermally stable poly(ester-imide)s containing different natural amino acids linkages. Journal of Polymer Research, **18**, 373–384 (2011). DOI: 10.1007/s10965-010-9427-z

[30] Chen J., Zhou Y., Nan Q., Ye X., Sun Y., Zhang F., Wang Z.: Preparation and properties of optically active polyurethane/TiO_2 nanocomposites derived from optically pure 1,1′-binaphthyl. European Polymer Journal, **43**, 4151–4159 (2007). DOI: 10.1016/j.eurpolymj.2007.07.006

[31] Chen J., Zhou Y., Nan Q., Sun Y., Ye X., Wang Zh.: Synthesis, characterization and infrared emissivity study of polyurethane/TiO_2 nanocomposites. Applied Surface Science, **253**, 9154–9158 (2007). DOI: 10.1016/j.apsusc.2007.05.046

[32] Higashi F., Ong C-H., Okada Y.: High-molecular-weight copolyesters of dihydroxybenzophenones by 'induced' copolyesterification using TsCl/DMF/Py as a condensing agent. Journal of Polymer Science Part A: Polymer Chemistry, **37**, 3625–3631 (1999). DOI: 10.1002/(SICI)1099-0518(19990915)37:18<3625::AID-POLA10>3.0.CO;2-V

[33] Higashi F., Akiyama N., Takahashi I., Koyama T.: Direct polycondensation of aromatic dicarboxylic acids and bisphenols with tosyl chloride and *N*,*N*-dimethylformamide in pyridine. Journal of Polymer Science: Polymer Chemistry Edition, **22**, 1653–1660 (1984). DOI: 10.1002/pol.1984.170220712

[34] Yao Q., Zhou Y., Sun Y., Ye X.: Synthesis of TiO_2 hybrid molecular imprinted polymer for ethofumesate linked by silane coupling agent. Journal of Inorganic and Organometallic Polymers, **18**, 477–484 (2008). DOI: 10.1007/s10904-008-9227-7

[35] Mallakpour S., Soltanian S.: Studies on syntheses and morphology characteristic of chiral novel poly(ester-imide)/TiO_2 bionanocomposites derived from l-phenylalanine based diacid. Polymer, **51**, 5369–5376 (2010). DOI: 10.1016/j.polymer.2010.09.063

[36] Nakayama N., Hayashi T.: Preparation and characterization of poly(L-lactic acid)/TiO_2 nanoparticle nanocomposite films with high transparency and efficient photodegradability. Polymer Degradation and Stability, **92**, 1255–1264 (2007). DOI: 10.1016/j.polymdegradstab.2007.03.026

[37] Van Krevelen D. W., Hoftyzer P. J.: Properties of polymers. Elsevier, Amsterdam (1976).

[38] Fujimura K., Miyake A.: The effect of specific surface area of TiO_2 on the thermal decomposition of ammonium perchlorate. Journal of Thermal Analysis and Calorimetry, **99**, 27–31 (2010). DOI: 10.1007/s10973-009-0462-0

[39] Chen Y., Yan L., Wang R., Fan H., Zhang Q.: Antimicrobial polyurethane synthetic leather coating with *in-situ* generated Nano-TiO_2. Fibers and Polymers, **11**, 689–694 (2010). DOI: 10.1007/s12221-010-0689-1